Journal of Hazardous Materials 199–200 (2012) 321–327

Contents lists available at SciVerse ScienceDirect

Journal of Hazardous Materials

journal homepage: www.elsevier.com/locate/jhazmat

Utilization of recycled cathode ray tubes glass in cement mortar for X-ray radiation-shielding applications

Tung-Chai Ling[a], Chi-Sun Poon[a,*], Wai-Shung Lam[a], Tai-Po Chan[b], Karl Ka-Lok Fung[b]

[a] Dep. of Civil and Structural Engineering, The Hong Kong Polytechnic University, Hung Hom, Kowloon, Hong Kong
[b] Department of Health Technology and Informatics, Hong Kong

ARTICLE INFO

Article history:
Received 2 June 2011
Received in revised form 31 October 2011
Accepted 4 November 2011
Available online 10 November 2011

Keywords:
Cathode ray tubes
Glass recycling
Cement mortar
Radiation-shielding
Density
Strength

ABSTRACT

Recycled glass derived from cathode ray tubes (CRT) glass with a specific gravity of approximately 3.0 g/cm^3 can be potentially suitable to be used as fine aggregate for preparing cement mortars for X-ray radiation-shielding applications. In this work, the effects of using crushed glass derived from crushed CRT funnel glass (both acid washed and unwashed) and crushed ordinary beverage container glass at different replacement levels (0%, 25%, 50%, 75% and 100% by volume) of sand on the mechanical properties (strength and density) and radiation-shielding performance of the cement–sand mortars were studied. The results show that all the prepared mortars had compressive strength values greater than 30 MPa which are suitable for most building applications based on ASTM C 270. The density and shielding performance of the mortar prepared with ordinary crushed (lead-free) glass was similar to the control mortar. However, a significant enhancement of radiation-shielding was achieved when the CRT glasses were used due to the presence of lead in the glass. In addition, the radiation shielding contribution of CRT glasses was more pronounced when the mortar was subject to a higher level of X-ray energy.

1. Introduction

1.1. Cathode ray tubes

The cathode ray tube (CRT) was first developed in 1897 by Ferdinand Braun as an oscilloscope to view and measure electrical signals [1]. Until the 1920s, the CRT was used as a medium to send and receive images electronically in television systems. Later, the concept of applying colour CRT was introduced in 1949.

A CRT consists of three basic parts: the electron gun (neck) assembly, the viewing surface (panel), and the glass envelope (funnel). The basic raw material in the CRT glass is silica (~50–60 wt.%). But other different metallic oxides such as barium oxide and lead oxide are required to be incorporated in CRT glass as shielding agents for harmful radiation [2]. The oxide content in each component part is slightly different. For instance, the panel glass only contains relatively low lead oxide content (0–3 wt.%), whereas a relatively high PbO content is often added to the funnel glass (22–25 wt.%) and the neck glass (~30 wt.%) parts to provide the required radiation shielding [3].

1.2. Management of cathode ray tubes

Electronic-waste disposal has become a global environmental problem. In the European Union, 80% of the total e-waste discarded in 2001 was CRT waste sourced from discarded TV and computer monitors [4]. In the United States, CRT made up one-third of the total e-waste quantity back in the year 1999 [5]. Predictions by a model [6] indicated that the mass of leaded glass required to be disposed of in the US may be 6 times the current mass by the year 2050. This is due to rapid developments in technology and the electronic products being replaced by newer models (high resolution LCD/LED monitor and TV sets) at a rapid rate. With little handling alternatives, discarded CRT derived from monitors and televisions are frequently sent to landfills.

A number of studies [7,8] demonstrated that the neck and funnel glasses of CRT can be considered hazardous waste due to its high content of lead and its potential leaching based on tested results of the toxicity characteristics leaching procedure (TCLP).

With rising awareness of the problems caused by Pb leaching from CRT, legislation in Europe and North America imposes stringent controls on CRT disposal. Also, alternatives other than landfilling are urgently required to offer a better management solution for dealing with CRT waste. Reuse by repair/redistribution may delay the rate of CRT waste generation, but its eventual disposal at the end of their life cycle remains a major concern.

* Corresponding author. Tel.: +852 2766 6024; fax: +852 2334 6389.
E-mail address: cecspoon@polyu.edu.hk (C.-S. Poon).

0304-3894/$ – see front matter © 2011 Elsevier B.V. All rights reserved.
doi:10.1016/j.jhazmat.2011.11.019

Table 1
Particle size distributions and physical properties of fine aggregates.

Sieve size and physical properties	Percentage passing (%)			
	River sand	Crushed funnel glass (CFG)	Treated funnel glass (TFG)	Crushed beverage glass (CBG)
2.36 mm	100	100	100	100
1.18 mm	94.8	71.4	65.7	53.5
0.6 mm	76.4	40.6	31.6	27.6
0.3 mm	29.2	15.3	8.4	12.7
0.15 mm	2.2	2.3	0.6	5.0
Fineness modulus	1.97	2.70	2.94	3.01
Relative density (g/cm^3)	2.62	3.00	2.99	2.49

Reuse of materials from CRT requires disassembly and sorting prior to utilization. According to the recycling experiences worldwide, electric cords, plastic casings, copper yokes and shadow masks are normally first removed to isolate the CRT. The glass components of CRT are then separated into separate parts and crushed into glass cullets [9]. Separation of funnel and panel glass is commonly performed by laser cutting or by a hot wire separation method [2].

Chemical treatments of the heavy metals on the CRT glass by using alkali and/or acid solutions have been investigated. Foresman and Foresman [10] claimed that a solution with (3 mass%) alkali hydroxides could remove lead on the surface of pulverized glass at a temperature of 70 °C when constantly stirred. Goforth et al. [11] also found that Pb can be extracted from a CRT funnel glass sample with a carbonate/bicarbonate buffer (pH 9). Ioannidis and Zouboulis [12] investigated Pb leaching by several acidic leaching solutions from hazardous industrial wastes and found that the nitric and acetic acid can efficiently remove more than 50% of Pb.

1.3. Research significance

Lead-based glasses have widely been used in diagnostic and medical applications, because of its good X-ray shielding ability to absorb various ranges of photon energies [13–15]. Due to environmental considerations of toxicity of lead, the use of other heavy-metals such as bismuth (Bi) and barium (Ba) to replace lead for the production of radiation shielding glasses has received much attention [16–19]. Further, a lead-free radiation protecting silicate glass containing Bi_2O_3 showed a good compatibility shielding properties in comparing with the glass containing PbO [20]. Moreover, Singh et al. [21] have determined that a barium–borate–flyash glass had better shielding properties than that of standard radiation shielding concrete. In the present work, we have investigated the potential use of recycled glass derived from CRT funnel glass (lead containing) as a fine aggregate in cement mortar for X-ray radiation-shielding applications. Three types of recycled glass were studied, namely crushed funnel glass (lead-leaded), treated funnel glass (metals from the surface of the crushed funnel glass particles are removed through an acid treatment process) and crushed beverage bottle glass (lead-free), so that a more comprehensive evaluation of the effect of different types of glass on the radiation-shielding properties can be obtained. Four replacement levels at 25%, 50%, 75% and 100% for sand by each type of glass for preparing the cement mortars were studied.

2. Experimental details

2.1. Materials

The materials used to prepare the mortar were ordinary Portland cement (OPC), fly ash and fine aggregate with a particle size of less than 2.36 mm.

2.1.1. Cementitious materials

ASTM Type I OPC and a fly ash complying with ASTM class F ash were used.

2.1.2. Aggregates

River sand having a fineness modulus of 1.33 was used as the natural fine aggregate in the control mix. Crushed CRT funnel glass (CFG, crushed and without acid treatment) and acid washed (treated) crushed CRT funnel glass (TFG) were used to replace sand by an equivalent volume method. The details of treatment process for the TFG have been reported in literature [22]. Conventional crushed beverage glass (CBG, lead-free) derived from post-consumer beverage container sources was also used for perform comparative studies. The particle size distributions and physical properties of all the fine aggregates used are presented in Table 1.

2.2. Mix proportions

A total of 13 mortar mixes were prepared in this study. All the cement mortars were prepared with a fixed cementitious material content of 608 kg/m^3. A sand-to-cementitious material ratio of 2.5 and a water-to-cementitious material ratio of 0.45 were used. The mix proportions of all the mortar mixes are shown in Table 2. As can be seen in the table, the mix design parameters for all the mortar mixes were kept constant except for the use of different types of fine aggregates. Three different types of recycled glass aggregates were used as a replacement (volume method) for an equal part of river sand at a level of 25%, 50%, 75% and 100%.

2.3. Mortar sample preparation

All the materials for the mortar mixes were put in and mixed for 5 min using a standard rotating drum type mixer. The freshly mixed materials were placed into steel moulds in two layers of approximately equal depth. After the first layer was filled, a rough compaction was applied by rodding the moulds 5 times uniformly over the cross section. After the second (final) layer was placed, the moulds were placed on a mechanical vibrating table for compaction.

All the specimens were covered with a plastic sheet in the laboratory at a temperature of 23 ± 3 °C immediately after casting. The specimens were demoulded after one day and then water cured for a further 27 days with an average temperature of 25 ± 3 °C before testing.

2.4. Size of test specimens and testing methods

The mortar specimens were cast in two types of moulds. Prism specimens having a dimension of 40 mm × 40 mm × 160 mm were used to determine the hardened density (water displacement method) according to BS 1881 Part 114 and flexural and equivalent compressive strength according to ASTM C348 and ASTM

Table 2
Mix proportions of mortar (kg/m^3).

No.	Mix notation	Cementitious			Fine aggregate			Water
		Cement	Fly ash	Sand	CFG	TFG	CBG	
1	Control mortar (CM)	456	152	1519	0	–	–	273
2	CFG25	456	152	1139	433	–	–	273
3	CFG50	456	152	759	867	–	–	273
4	CFG75	456	152	380	1300	–	–	273
5	CFG100	456	152	0	1734	–	–	273
6	TFG25	456	152	1139	–	433	–	273
7	TFG50	456	152	759	–	867	–	273
8	TFG75	456	152	380	–	1300	–	273
9	TFG100	456	152	0	–	1734	–	273
10	CBG25	456	152	1139	–	–	361	273
11	CBG50	456	152	759	–	–	722	273
12	CBG75	456	152	380	–	–	1083	273
13	CBG100	456	152	0	–	–	1446	273

C349, respectively. All the results reported are the averages of three measurements.

For each mortar mix, five additional mortar disc samples with a dimension of 100 mm × 100 mm × 5 mm were cast for the evaluation of the radiation-shielding properties.

2.5. X-ray radiation-shielding test

The X-ray radiation-shielding test was performed in an X-ray laboratory designed for medical diagnostic examination. The laboratory was installed with a medium frequency X-ray unit (Toshiba, KXO-30R). Quality assurance tests for this unit are performed regularly. These tests include output reproducibility, kVp accuracy and kVp reproducibility. Recent results confirmed the very good performance of this X-ray source with the coefficient of variation for all these tests being less than 2%. The projected distance (F) between the target of the diagnostic X-ray tube (DXB-0324CS-A) and the test samples was kept at 700 mm. Collimators with double layers of lead plates/leaves was positioned below the X-ray tube head for confining/controlling the primary beam. The beam size projected onto the 100 mm × 100 mm mortar plate (absorber) was 60 mm × 60 mm. Based on the projected distance (F = 700 mm) and semi beam size (b = 60/2 mm), the angular narrow beam width of θ = 2.45° was determined, according to $b = F \sin\theta$ mathematic relationship. This angle value is within the scatter acceptance angles value of 3.57° proposed by Singh et al. [23]. Hence, the scattering effect due to the probability of scattered photons reaching the Chamber could be very small. Furthermore, to ensure dose at a point in free air beneath the samples can be measured accurately, a 6-cc Ionization Chamber was positioned 100 mm beneath the absorber to avoid any scatter radiation reaching to the detector. Fig. 1 shows respectively the schematic diagram and the photograph of the experimental test setup used for this study.

3. Results and discussion

3.1. Flexural and compressive strengths of mortar

The 28-day flexural and compressive strength of the mortar mixes are shown in Fig. 2. It can be seen that the control mortar with

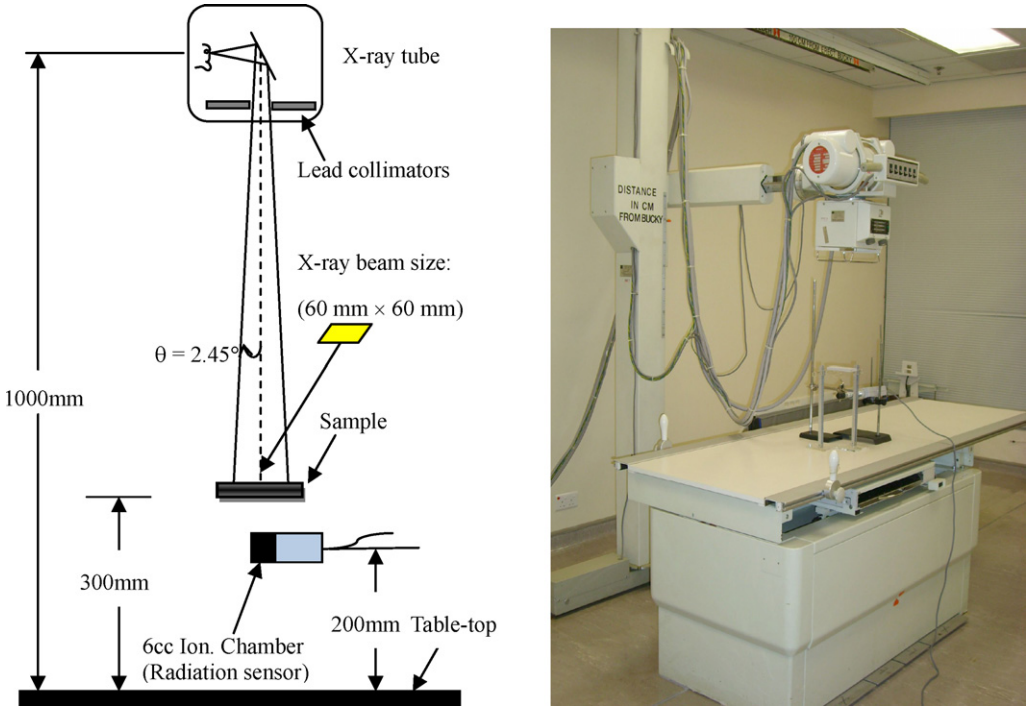

Fig. 1. Schematic diagram of the experimental setup of X-ray radiation-shielding tests.

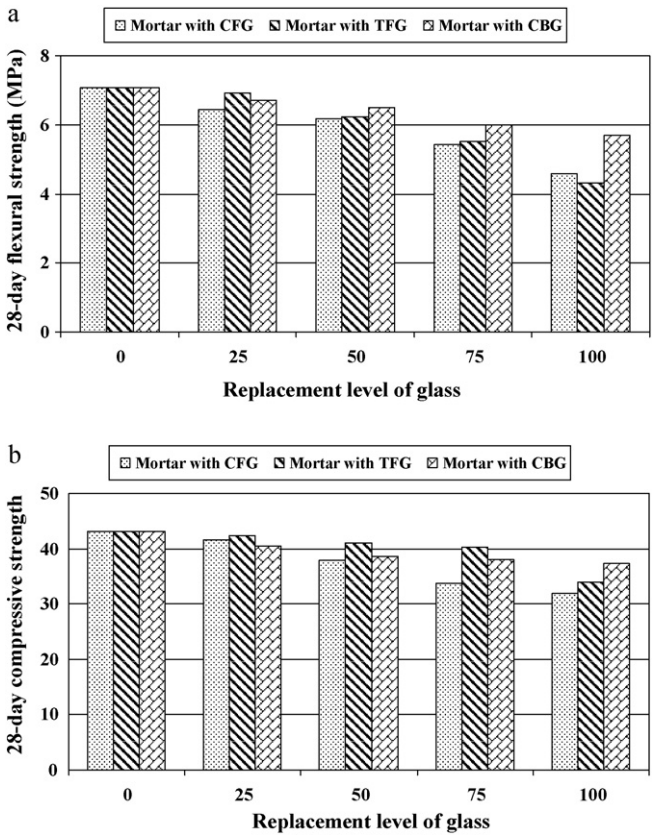

Fig. 2. 28-day (a) flexural and (b) compressive strength of mortars.

100% sand, in general, had higher flexural and compressive strength values than the other mortar mixes prepared with the different types of glass. The strength decreased with increasing glass content probably due to the weaker adhesion between the smooth surface of the glass particles and the cement mortar [24,25]. However, the strength values of all mortar mixes were within the strength limits stipulated by the Building (Construction) Regulations – Chapter 123 Hong Kong and ASTM C 270.

3.2. Hardened density of mortar

Fig. 3 shows the effect of CFG, TFG and CBG content on the hardened density of the mortars. It can be clearly shown that the hardened density of the mortars increased with increasing CFG and TFG content. At 100% replacement, the density of the CFG and TFG mortars increased by 14.6% and 11.2% as compared to the control

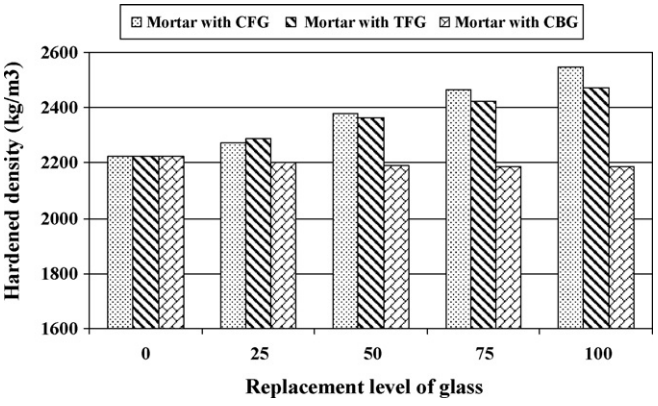

Fig. 3. Hardened density of mortars.

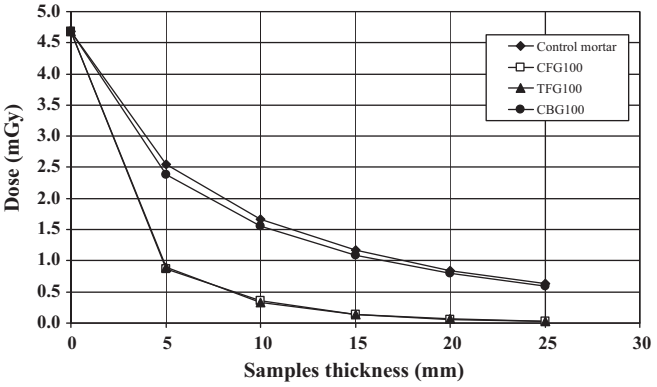

Fig. 4. Dose attained beneath the mortars prepared with different types of glass.

mix, respectively. The significant contribution of lead in the glass to the mortar's density is evident. However, due to the removal of lead on the surface of TFG through the acid washing process, the density of TFG mortar was lower than that of CFG mortar for the same glass replacement content. As expected, the density of the CBG mortar slightly decreased with increase of CBG content. This was due to the specific gravity of CBG being lower than that of sand (see Table 1).

3.3. X-ray radiation-shielding properties

3.3.1. Effect of different types of recycled glass

Fig. 4 compares the radiation attenuation results of the control mortar and the mortars prepared with different types of glass at an X-ray energy level of 140 kVp (peak kilovoltage). The exit air dose value was attained directly beneath the samples. From the results obtained, it is clearly shown that different types of aggregate and thickness of the mortar samples absorbed different amounts of X-ray radiation.

The lowest dose value was recorded for the CFG100 mix. The dose attained beneath the 5 mm thick CFG mortar was 56.2% lower than the corresponding control mortar. This result can be attributed to the fact that the CFG mortar has a higher density. The atomic structure in the dense CFG particles actively interacted with X-rays, thus reducing its energy and the depth of radiation penetration [26].

The results show that the dose values were also greatly dependent on the sample thickness. As the sample thickness was increased from 5 mm to 25 mm, the doses attained progressively reduced. This result is in agreement with pervious findings of Asai and Hirayama [27]. It is well known that increasing the thickness of absorber might increase the buildup factor due to a multiple scattering effect. However, the photoelectric effect would be predominance at this energy level (140 kVp) which resulted in the fast removal of the low energy photons to avoid their buildup in the medium [28]. Also, a study of Singh et al. [23] have demonstrated that a well collimated narrow beam with a small angular can suppress the multiple scattered photons effect even at large absorber thickness of 4 mfp (mean free path). Thus it can be concluded that both increasing the material's density and sample thickness can provide a higher radiation-shielding effect.

3.3.2. Influence of glass content

The influence of different glass content on radiation-shielding was investigated and the results are plotted in Fig. 5. It is noted that the increase of CBG content had no significant effect on the dose value due to it having a similar density to that of sand.

However, the dose value decreased with increasing CFG and TFG content in the mortars. It is obvious that the denser leaded CRT aggregates increased the effectiveness of radiation-shielding

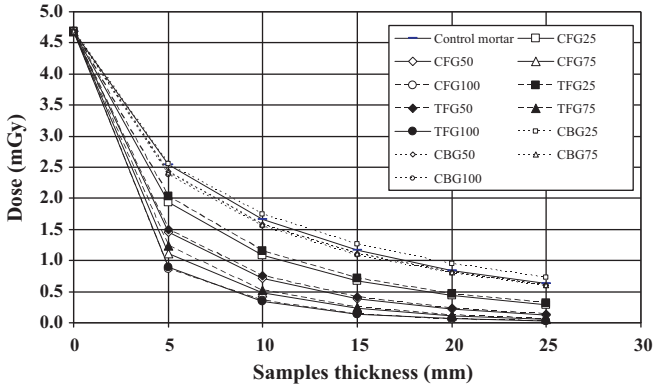

Fig. 5. Dose attained beneath the mortars with different sample thickness.

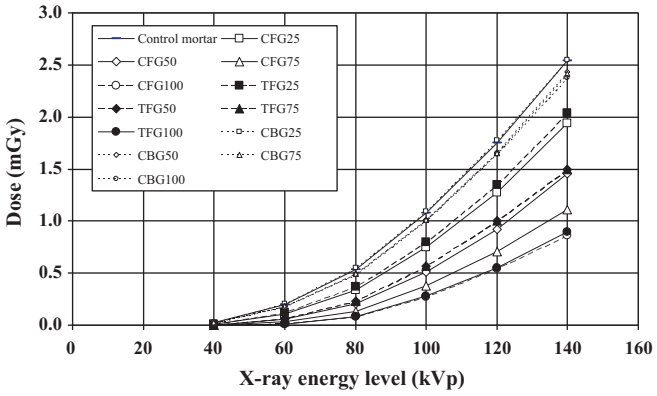

Fig. 7. Effect of energy level on dose attained beneath the 5 mm thick mortar samples.

because they can absorb more radiation photons. Comparing the results of the CFG and TFG mortars, the positive contribution of CFG on radiation-shielding became less pronounced as the mortar thickness increased.

As the density of a material determines its resistance to radiation penetration, thus it is of interest to plot the dose values as a function of the density of the mortar samples (Fig. 6). There is a strong linear relationship between the two, with the dose values decreasing linearly with increasing density of the mortar samples.

3.3.3. *Influence of X-ray energy level*

To investigate the possibility of application of the CRT mortar-based shielding materials in areas such as diagnostic X-ray and CT-scanner facilities, the radiation-shielding ability of the mortars was tested with varying X-ray energy level ranging from 40 kVp to 140 kVp, with an increment of 20 kVp and an exposure time of about 20 mAs. The results are presented in Fig. 7.

It can be seen that the dose values varied with X-ray energy level. This is because the doses attained can be associated with the different energy absorption mechanisms for different energy levels [29]. At this region of low energies, the contribution from photoelectric interactions is more important than Compton scattering. The Compton scattering can be ignored in our experiment due to its small effect and only predominate at higher energies (few MeV) [30].

As can be seen in Fig. 7, for 40 kVp energy investigation the X-rays have a very low energy and were absorbed within 5 mm thick mortar absorber, regardless of types of aggregate. However, the measured dose increased rapidly with increasing energy level which might be related to the decrease of the probability of photoelectric interactions (attenuation). At higher range of energies (120–140 kVp), the measured dose of the leaded glass (CFG or TFG) mortars were clearly different from those (sand or CBG) mortars. This indicates the photoelectric interaction/attenuation for the CFG and TFG at these energies were much higher in comparing with both the sand CBG. It is also noted that, increasing the CFG and TFG contents in the cement mortar significantly improved the radiation-shielding properties, particularly at higher energy levels. However, the CBG mortar had similar dose values to that of the control, regardless of the glass replacement and energy level.

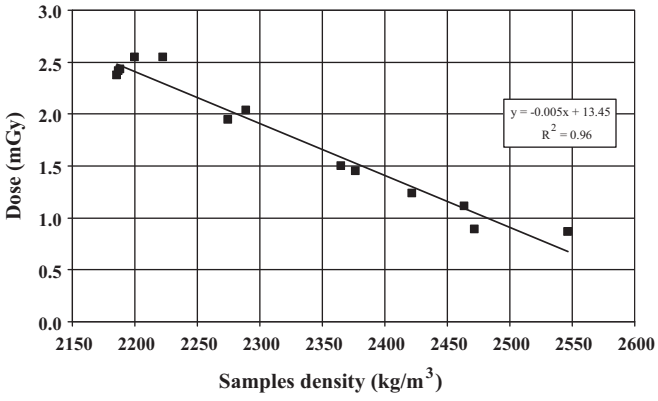

Fig. 6. Dose values as a function of mortar density for different compositions.

3.3.4. *Linear attenuation coefficients, half-value layer, tenth-value layer thickness of mortar-based shielding compositions*

As discussed in the previous section, the depth of X-ray penetration for a given energy level is dependent on the density of the mortar samples. Since different materials have different radiation attenuation abilities, a convenient method to compare the required thickness of the mortar samples for effective radiation shielding was used and the results are shown in Fig. 8 and Table 3. The method compares the equivalent shielding thickness in terms of half-value layer (HVL) and tenth-value layer (TVL) of the mortar-based shielding composites at an X-ray energy level of 140 kV with that of a 1 mm thick lead sheet.The linear attenuation coefficients (LAC) were determined using the following

$$\mu = \frac{1}{\chi} \ln\left(\frac{I_0}{I}\right) \quad (1)$$

Table 3
Linear attenuation coefficients, HVL and TVL of mortars at energy level of 140 kV.

Sample	Linear attenuation coefficient (mm^{-1})	Thickness (mm) 1 mm Lead Eq.	HVL (mm)	TVL (mm)
Lead sheet[a]	4.010	1.0	0.2	0.6
CM	0.069	57.7	10.0	33.1
CFG25	0.095	42.4	7.3	24.3
CFG50	0.121	33.2	5.7	19.1
CFG75	0.145	27.6	4.8	15.9
CFG100	0.171	23.4	4.0	13.4
TFG25	0.093	43.0	7.4	24.7
TFG50	0.118	34.1	5.9	19.6
TFG75	0.146	27.4	4.7	15.7
TFG100	0.167	24.1	4.2	13.8
CBG25	0.063	63.8	11.0	36.6
CBG50	0.069	58.2	10.1	33.4
CBG75	0.069	58.1	10.1	33.4
CBG100	0.069	58.5	10.1	33.6

[a] Lead sheet (1 mm Lead Equivalent).

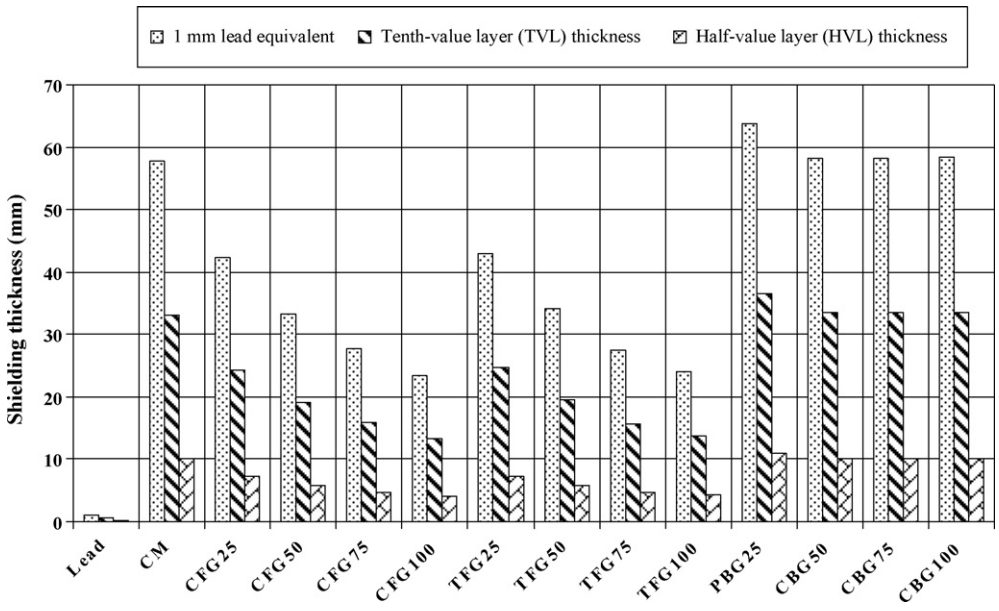

Fig. 8. Comparison of radiation-shielding thickness of mortars with 1 mm lead sheet.

where the χ is the sample thickness and I_0 and I are the number of dose counts (intensity) recorded in the primary beam and detector beneath the sample, respectively.

The HVL and TVL are the thickness of the samples at which the incident energy is attenuated by a factor of one-half and one-tenth, respectively. Thus, from Eq. (1) the value of HVL and TVL are given by $(\ln 2)/\mu$ and $(\ln 10)/\mu$, respectively.

As can be seen from the figure, no significant difference was noticed for the mortar prepared with different CBG content. For the CFG and TFG, as the glass content incorporated in the mortar increased from 0 to 100%, the HVL values decreased from 10 cm to 4.0 cm and 4.2 cm, respectively. This means that the material needed for the CFG and TFG mortars to reduce the dose rate by one-half, were only 40% and 42% of the material required for the control mortar. Therefore, it may be of economic and practical value to use the CFG and TFG mortar as a shielding material for diagnostic X-ray and CT-scanner rooms.

4. Conclusion

Based on the laboratory investigation, the following conclusions can be drawn:

- The flexural and compressive strength gradually reduces with increasing glass content, regardless of the type of glass. However, all the mortar mixes showed strength values greater than 4 MPa (flexural strength) and 30 MPa (compressive strength), which can be used for most building applications.
- The crushed beverage bottle glass (CBG) has no significant influence on the density and radiation-shielding performance of the mortar when compared with the control (sand) mortar.
- The hardened density of the mortar increases with increasing crushed funnel glass (CFG) and treated funnel glass (TFG) content because of the higher specific gravity of the leaded CRT glass.
- The radiation-shielding properties are significantly improved by the incorporation of CFG and TFG as aggregates.
- It is feasible to utilize CFG and TFG as aggregates in mortar-based composites for various shielding applications such as in diagnostic X-ray and CT-scanner rooms.

Acknowledgments

The authors would like to thank the Environment and Conservation Fund and the Woo Wheelock Greed Fund, and The Hong Kong Polytechnic University for funding support.

References

[1] J. Leigh, A. Johnson, L. Renambot, Chapter 2 advances in computer displays, Adv. Comput. 77 (2009) 57–77.
[2] C.H. Lee, C.T. Chang, K.S. Fan, T.C. Chang, An overview of recycling and treatment of scrap computers, J. Hazard. Mater. 114 (1–3) (2004) 93–100.
[3] J.H. Connelly, D.J. Lopata, CRTs and TV picture tubes, in: Engineered Materials Handbook, Vol. 4: Ceramics and Glasses, ASM International, 1991, pp. 1038–1044.
[4] C. Gable, B. Shireman, Computer and electronic product stewardship: are we ready for the challenge? Environ. Qual. Manage. 11 (1) (2001) 35–45.
[5] T.G. Townsend, S.E. Musson, Y.C. Jang, I.H. Chung, Characterization of lead leachability from cathode ray tubes using the toxicity characteristics leaching procedure, Environ. Sci. Technol. 34 (20) (2000) 4376–4381.
[6] J.D. Linton, J.S. Yeomans, The role of forecasting in sustainability, Technol. Forecast. Soc. Change 70 (1) (2000) 21–38.
[7] C.H. Lee, C.S. His, Recycling of scrap cathode ray tubes, Environ. Sci. Technol. 36 (1) (2002) 69–75.
[8] Y.C. Jang, T.G. Townsend, Leaching of lead from computer printed wire boards and cathode ray tubes by municipal solid waste landfill leachates, Environ. Sci. Technol. 37 (20) (2003) 4778–4784.
[9] T. Matsuto, C.H. Jung, N. Tanaka, Material and heavy metal balance in a recycling facility for home electrical appliances, Waste Manag. 24 (5) (2003) 425–436.
[10] G. Foresman, J.A. Foresman, Method for removing lead from coated glass, European Patent Office, Publication Number: WO0020121, 2000.
[11] D.E. Goforth, L.R. Morse, S.T. Gulati, Lead extraction from CRT glasses, in: SID International Symposium Digest of Technical Papers, SID, USA, 1994, p. 905.
[12] A. Th. Ioannidis, A.I. Zouboulis, Selective removal of lead and bromide from a hazardous industrial solid waste using Limited Acid Demand and Separation Factor at ambient conditions, J. Hazard. Mater. 131 (1–3) (2006) 46–58.
[13] M. Kurudirek, Y. Ozdemir, O. Simsek, R. Durak, Comparison of some lead and non-lead based glass systems, standard shielding concretes and commercial window glasses in terms of shielding parameters in the energy region of 1 keV–100 GeV: a comparative study, J. Nucl. Mater. 407 (2) (2010) 110–115.
[14] K. Kirdsiri, J. Kaewkhao, A. Pokaipisit, W. Chewpraditkul, P. Limsuwan, Gamma-rays shielding properties of xPbO:$(100-x)B_2O_3$ glasses system at 662 keV, Ann. Nucl. Energy 36 (6) (2009) 1360–1365.
[15] S.R. Manohara, S.M. Hanagodimath, L. Gerward, Photon interaction and energy absorption in glass: a transparent gamma ray shield, J. Nucl. Mater. 393 (15) (2009) 465–472.
[16] K.J. Singh, N. Singh, R.S. Kaundal, K. Singh, Gamma-ray shielding and structural properties of PbO–SiO_2 glass, Nucl. Instrum. Methods B 266 (6) (2008) 944–948.

[17] N. Singh, K.J. Singh, K. Singh, H. Singh, Comparative study of lead borate and bismuth lead borate glass system as gamma-radiation shielding materials, Nucl. Instrum. Methods B 225 (3) (2004) 305–309.
[18] N. Singh, K.J. Singh, K. Singh, H. Singh, Gamma-ray attenuation studies of $PbO–BaO–B_2O_3$ glass system, Radiat. Meas. 41 (1) (2006) 84–88.
[19] K. Singh, H. Singh, G. Sharma, L. Gerward, A. Khanna, R. Kumar, R. Nathuram, H.S. Sahota, Gamma-ray shielding properties of $CaO–SrO–B_2O_3$ glasses, Radiat. Phys. Chem. 72 (6) (2005) 225–228.
[20] K. Kirdsiri, J. Kaewkhao, N. Chanthima, P. Limsuwan, Comparative study of silicate glasses containing Bi_2O_3, PbO and BaO: radiation shielding and optical properties, Ann. Nucl. Energy 38 (6) (2011) 1438–1441.
[21] S. Singh, A. Kumar, D. Singh, K.S. Thind, G.S. Mudahar, Barium–borate–flyash glasses: As radiation shielding materials, Nucl. Instrum. Methods B 266 (1) (2008) 140–146.
[22] T.C. Ling, C.S. Poon, Utilization of recycled glass derived from cathode ray tube glass as fine aggregate in cement mortar, J. Hazard. Mater. 192 (2) (2011) 451–456.
[23] S. Singh, A. Kumar, C. Singh, K.S. Thind, G.S. Mudahar, Effect of finite sample dimensions and total scatter acceptance angle on the gamma ray buildup factor, Ann. Nucl. Energy 35 (12) (2008) 2414–2416.
[24] T.C. Ling, C.S. Poon, Properties of architectural mortar prepared with recycled glass with different particle sizes, Mater. Design. 32 (5) (2011) 2675–2684.
[25] S.C. Kou, C.S. Poon, Properties of self-compacting concrete prepared with recycled glass aggregate, Cem. Concr. Compos. 31 (2) (2009) 107–113.
[26] R. Nath, N. Yue, L. Liu, On the depth of penetration of photons and electrons for intravascular brachytherapy, Cardiovasc. Radiat. Med. 1 (1) (1999) 72–79.
[27] J. Asai, H. Hirayama, Dose estimates for an insertion device beamline with a tapered absorber at the Canadian Light Source, Radiat. Meas. 46 (4) (2011) 418–424.
[28] D. Calabrese, A.M. Covington, J.S. Thompson, Production of group IIA atomic and molecular negative ion beams in a cesium-sputter negative ion source, Nucl. Instrum. Methods Phys. Res. A 379 (2) (1996) 192–195.
[29] L. Machenil, M. Vanderhaeghen, J. Ryckebusch, M. Waroquier, Absorption mechanisms in photon induced two-body knockout, Phys. Lett. B 316 (1) (1993) 17–22.
[30] U. Kaur, J.K. Sharma, P.S. Singh, T. Singh, Comparative studies of different concretes on the basis of some photon interaction parameters, Appl. Radiat. Isotopes (2011), doi:10.1016/j.apradiso.2011.07.011.